

# Force Titrations and Ionization State Sensitive Imaging of Functional Groups in Aqueous Solutions by Chemical Force Microscopy

Dmitri V. Vezenov, Aleksandr Noy, Lawrence F. Rozsnyai, and Charles M. Lieber\*

Contribution from the Department of Chemistry and Chemical Biology, Harvard University, Cambridge, Massachusetts 02138

Received September 26, 1996<sup>⊗</sup>

**Abstract:** Chemical force microscopy (CFM) was used to probe interactions between ionizable and neutral functional groups in aqueous solutions. Force microscope probe tips and sample substrates have been covalently modified with self-assembled monolayers (SAMs) terminating in distinct functional groups. SAMs were prepared by treating Au-coated or uncoated tips and substrates with functionalized thiols or silanes, respectively. A force microscope has been used to characterize adhesive and frictional interactions between probe tips and substrates modified with SAMs that terminate in  $-\text{NH}_2$ ,  $-\text{COOH}$ ,  $-\text{OH}$ , and  $-\text{CH}_3$  functional groups as a function of solution pH and ionic strength. In general, adhesion and friction forces were observed to depend on the chemical identity of the tip and sample surface and also were found to be highly sensitive to the changes in the ionization state of the terminal functionalities induced by varying the solution pH. Adhesion measurements made as a function of pH (force titrations) on amine-terminated surfaces exhibit a sharp decrease in the adhesion force at pH values below 4.5. The  $\text{p}K_{\text{a}}$  estimated from this drop in adhesion, which is due to the protonation of amine groups on the sample and tip, 3.9, is similar to the value determined by conventional contact angle wetting studies of these same surfaces. The large decrease in the  $\text{p}K$  of the amine group relative to homogeneous solution was attributed to the relatively hydrophobic environment of the amine group in these SAMs. Adhesion measurements made as a function of pH on  $-\text{COOH}$ -terminated surfaces exhibited a large drop in adhesion force for pH values greater than 5. The  $\text{p}K_{\text{a}}$  estimated from these data, 5.5, is similar to the free aqueous solution value. In addition, the adhesion force between nonionizable  $-\text{OH}$  and  $-\text{CH}_3$  groups was found to be independent of solution pH. The measured adhesive forces were interpreted using a contact mechanics model that incorporated the effects of the double layer free energy. Analyses of repulsive electrostatic forces and adhesion data recorded as a function of ionic strength were used to determine properties of the double layer. The pH dependence of the friction force between tips and samples modified with SAMs terminating in  $-\text{COOH}$ ,  $-\text{OH}$ , and  $-\text{CH}_3$  groups was measured as a function of applied load. For a given pH, these data exhibit a linear dependence on load with the slope corresponding to the coefficient of friction. The coefficient of friction for  $-\text{OH}$  and  $-\text{CH}_3$  groups was independent of pH, while the friction coefficient for  $-\text{COOH}$ -terminated surfaces drops significantly at a pH corresponding to the  $\text{p}K_{\text{a}}$  determined by adhesion measurements. The pH-dependent changes in friction forces for ionizable groups were exploited to map spatially changes in ionization state on surfaces terminating in  $-\text{COOH}$  and  $-\text{OH}$  functional groups.

## Introduction

Intermolecular forces impact a wide variety of problems in condensed phases ranging from ones relevant in materials science, such as adhesion, interfacial fracture, friction and boundary lubrication,<sup>1</sup> to those critical in biology such as signal transduction<sup>2</sup> and membrane assembly.<sup>3</sup> The key interactions controlling these phenomena can be broken down into fundamental types of chemical forces including van der Waals, hydrogen bonding, and electrostatic.<sup>3</sup> In many cases, these interactions are highly specific. In proteins, substitution of a single amino acid can completely change folding or lead to a large change in binding constant.<sup>4,5</sup> Studies have also shown that a change in the ionization state of a functional group in a

biomolecule can affect its interactions with neighboring groups and lead to a major change in overall structure.<sup>4,5</sup> For example, dramatic conformational changes in protein structures can be induced by small pH variations.<sup>5</sup> Since such biological processes take place in aqueous media, it is expected that the ability to detect, map, and interpret intermolecular interactions in this medium with chemical sensitivity on a microscopic scale will help to provide an understanding of these processes at the molecular level.

Atomic force microscopy (AFM) has recently emerged as a promising technique for both measuring intermolecular forces and imaging.<sup>6</sup> Key features of AFM include the ability to make local measurements with very high sensitivity and precision and to generate spatial maps of surface topography and surface forces. Intermolecular forces can also be measured with great sensitivity using the surface force apparatus (SFA),<sup>7</sup> interfacial force microscopy,<sup>8</sup> colloid probe microscopy,<sup>9</sup> and optical tweezers,<sup>10</sup> although these techniques cannot be used to provide

<sup>⊗</sup> Abstract published in *Advance ACS Abstracts*, February 1, 1997.

(1) (a) *Handbook of Micro/Nano Tribology*, 1st ed.; Bhushan, B., Ed.; CRC Press: Boca Raton, FL, 1995. (b) Kendall, K. *Science* **1994**, 263, 1720.

(2) (a) Weng, Z.; Rickles, R. J.; Feng, S.; Richard, S.; Shaw, A. S.; L. Schreiber, S.; Brugge, J. S. *Mol. Cell. Biol.* **1995**, 15, 5627. (b) Feng, S.; Chen, J. K.; Yu, H.; Simon, J. A.; Schreiber, S. L. *Science* **1994**, 266, 1241.

(3) Israelachvili, J. *Intermolecular and Surface Forces*; Academic Press: New York, 1992.

(4) Fersht, A. *Enzyme Structure and Mechanics*; W. H. Freeman: New York, 1985.

(5) Creighton, T. E. *Proteins: Structure and Molecular Properties*, 2nd ed.; W. H. Freeman: New York, 1993.

(6) Quate, C. *Surf. Sci.* **1994**, 299/300, 980.

(7) Israelachvili, J. *Acc. Chem. Res.* **1987**, 20, 415.

(8) Joyce, S.; Houston, J. *Rev. Sci. Instrum.* **1991**, 62, 710.

high-resolution spatial maps of forces. Because of the importance in mapping surface interactions to a variety of problems, we recently introduced a concept of chemical force microscopy (CFM)<sup>11,12</sup> that exploits specifically functionalized AFM tips to study intermolecular interactions on a nanometer scale. This approach allows us to control the chemical identity and surface energy of the probe by covalently linking a self-assembled monolayer (SAM) terminating in a distinct functional group to the tip surface. Chemical modification of the AFM probes eliminates uncertainties in terminal functionality associated with using an unmodified and often contaminated tip and allows us to study interactions between chosen distinct pairs of functional groups. Another advantage of CFM methodology is the flexibility in varying the tip chemistry, since organic monolayers terminating in virtually every possible functional group can be prepared using well-developed methods. Combining these features with the sensitivity and resolving power of AFM yields a technique capable of studying intermolecular interactions on a nanometer scale and AFM imaging with chemical sensitivity. The general ideas of CFM have been confirmed by several groups:<sup>13</sup> chemical specificity in adhesive forces was quantitatively studied in dry nitrogen environments<sup>13c</sup> and in solvents,<sup>13b,e</sup> and furthermore, chemical specificity of friction forces has been exploited to image functional group arrays in dry argon<sup>13a</sup> and ambient air.<sup>13d</sup>

This paper centers on using functionalized AFM probes to study interactions in aqueous solutions. Investigations in aqueous solution are especially important at this time in light of the increasing use of AFM to study biological systems.<sup>14</sup> Previous AFM studies have found that the images of biomolecules are highly sensitive to adhesion forces,<sup>15</sup> and that adhesion forces can be sensitive to solution ionic strength<sup>16</sup> and pH<sup>17</sup> and surface composition.<sup>18</sup> However, it has not been possible to provide a detailed understanding of the interactions from these AFM studies due to uncertainties in the tip–surface chemistry. On the other hand, the SFA and colloid probe microscopy have been used to study electrostatic interactions between relatively well-defined but large surfaces as a function of pH and ionic strength.<sup>19–23</sup> These latter studies suggest that by controlling the surface chemistry of the probe tip it should be possible to probe quantitatively electrostatic interactions in

aqueous solution. Recent studies employing tips coated with physisorbed phospholipids<sup>24</sup> and electroactive polymers and SAMs<sup>25</sup> confirm the potential for such an approach.

Herein we present systematic studies that probe interactions between tips and surfaces functionalized with SAMs terminating in ionizable and nonionizable functional groups in aqueous solutions. The adhesive and frictional forces in these systems are shown to depend in a predictable way on the ionization state of the terminal functionalities. On the basis of this dependence, a novel method of *force titration* is introduced for highly local characterization of the pK values of surface functional groups. Adhesion data are corroborated by macroscopic contact angle measurements and agree well with a double layer interaction model. In addition, we show that lateral forces follow the same trend as adhesion forces. This correlation is then used for ionization state-specific mapping of functional group distributions on surfaces. Implications of these results for research in chemistry and biology are discussed.

## Experimental Section

**Materials.** Bis(11-(4-azidobenzoato)-1-undecyl)disulfide (**I**), 11-mercaptopundecanoic acid, ethyl 4-aminobutyrate, and 11-mercaptopundecanol were available from previous studies.<sup>11</sup> Commercial octadecanethiol, (3-aminopropyl)triethoxysilane (APTES), potassium *tert*-butoxide (Aldrich), and mono-, di-, and tribasic sodium phosphates (Fisher Scientific) were used as received. Dibutylamine and diethanolamine (Aldrich) were distilled under reduced pressure and stored under N<sub>2</sub>. Solvents used in chemical manipulations were of reagent grade or better; solvents used in substrate and probe tip functionalization were HPLC grade to reduce particulate matter. All water was deionized (DI H<sub>2</sub>O) with a Barnstead NANOpure II filtration unit to 18 MΩ·cm resistivity.

Constant ionic strength buffer solutions were prepared by mixing 0.01 M mono-, di-, and tribasic sodium phosphate stock solutions in different proportions. The concentrations of all ions were calculated on the basis of measured pH and known values of dissociation constants of phosphoric acid.<sup>33</sup> Accordingly, the solutions were further diluted to give a final ionic strength of 0.01 M. Solutions of different ionic strength (from 10<sup>-2</sup> to 10<sup>-5</sup> M) were obtained by dilution of 0.01 M pH 7.2 buffer.

**Au-Coated Substrates and Probe Tips.** Si(100) wafers (Silicon Sense, Nashua, NH; test grade, 525 μm thick) and commercial Si<sub>3</sub>N<sub>4</sub> tip–cantilever assemblies (Digital Instruments, Santa Barbara, CA) were coated in an electron beam evaporator (base pressure 1 × 10<sup>-7</sup> Torr) with a 20 Å adhesion layer of Ti followed by 1000 Å of Au deposited at 1.5 Å/s.

**Substrate and Tip Modification.** Monolayers of **I** were formed by immersion of the Au-coated substrates and tips in 2–3 mM cyclohexane solutions for at least 12 h. Monolayers of 11-mercaptopundecanoic acid, octadecanethiol, and 11-mercaptopundecanol were formed by immersion of the substrates and probe tips in 2–3 mM EtOH solutions for at least 2 h. Before use or characterization, all SAM substrates were rinsed in EtOH (SAM substrates of **I** were first rinsed with cyclohexane and then EtOH) and dried with a stream of dry N<sub>2</sub>. Amine-terminated monolayers were prepared by immersing freshly cleaned Si(100) substrates and Si<sub>3</sub>N<sub>4</sub> tip–cantilever assemblies (piranha solution 1:2 H<sub>2</sub>SO<sub>4</sub>/H<sub>2</sub>O<sub>2</sub>, 90 °C, 20 min) in a 20 mM toluene solution of APTES for 2 h. Silane monolayer formation was verified by X-ray

(9) (a) Ducker, W. A.; Senden, T. J.; Pashley, R. M. *Nature* **1991**, 353, 239. (b) Ducker, W. A.; Senden, T. J.; Pashley, R. M. *Langmuir* **1992**, 8, 1831.

(10) (a) Ashkin, A.; Dziedzic, J. M.; Bjorkholm, J. E.; Chu, S. *Opt. Lett.* **1986**, 11, 288. (b) Kuo, S. C.; Sheetz, M. P. *Science* **1993**, 260, 232. (c) Svoboda, K.; Schmidt, C. F.; Schnapp, B. J.; Block, S. M. *Nature* **1993**, 365, 721. (d) Perkins, T.; Smith, D. E.; Chu, S. *Science* **1994**, 264, 819. (e) Finer, J. T.; Simmons, R. M.; Spudich, J. A. *Nature* **1994**, 386, 113.

(11) Frisbie, C. D.; Rozsnyai, L. F.; Noy, A.; Wrighton, M. S.; Lieber, C. M. *Science* **1994**, 265, 2071.

(12) Noy, A.; Frisbie, C. D.; Rozsnyai, L. F.; Wrighton, M. S.; Lieber, C. M. *J. Am. Chem. Soc.* **1995**, 117, 7943.

(13) (a) Green, J.-B.; McDermott, M. T.; Porter, M. D.; Siperko, L. M. *J. Phys. Chem.* **1995**, 99, 10960. (b) Han, T.; Williams, J. M.; Beebe, Jr., T. P. *Anal. Chim. Acta* **1995**, 307, 365. (c) Thomas, R. C.; Houston, J. E.; Crooks, R. M.; Kim, T.; Michalske, T. A. *J. Am. Chem. Soc.* **1995**, 117, 3830. (d) Akari, S.; Horn, D.; Keller, H.; Schrepp, W. *Adv. Mater.* **1995**, 7, 549. (e) Sinniah, S. K.; Steel, A. B.; Miller, C. J.; Reutt-Robey, J. E. *J. Am. Chem. Soc.* **1996**, 118, 8925.

(14) For a recent review on high resolution AFM in biology see: Shao, Z.; Yang, J. Q. *Rev. Biophys.* **1995**, 28, 195.

(15) Lyubchenko, Y. L.; Oden, P. I.; Lampner, D.; Lindsay, S. M.; Dunker, K. A. *Nucleic Acids Res.* **1993**, 21, 1117.

(16) (a) Weisenhorn, A. L.; Maivald, P.; Butt, H.-J.; Hansma, P. K. *Phys. Rev. B* **1992**, 45, 11226. (b) Butt, H.-J. *Biophys. J.* **1991**, 60, 1438.

(17) Werf, K. O. v. d.; Putman, C. A. J.; Grooth, B. C. d.; Greve, J. *Appl. Phys. Lett.* **1994**, 65, 1195.

(18) Ishino, T.; Hieda, H.; Tanaka, K.; Gemma, N. *Jpn. J. Appl. Phys.* **1994**, 33, 4718.

(19) Claesson, P. M.; Blomberg, E.; Froberg, J. C.; Nylander, T.; Arnebrant, T. *Adv. Colloid Interface Sci.* **1995**, 57, 161.

(20) (a) Larson, D.; Drummond, C. J.; Chan, D. Y. C.; Grieser, F. J. *Phys. Chem.* **1995**, 99, 2114. (b) Meagher, L.; Pashley, R. M. *Langmuir* **1995**, 11, 4019.

(21) Johnson, S. B.; Drummond, C. J.; Scales, P. J.; Nishimura, S. *Langmuir* **1995**, 7, 2367.

(22) Vigh, E.; Xu, Z.; Steinberg, S.; Israelachvili, J. J. *Colloid Interface Sci.* **1994**, 165, 367.

(23) Pashley, R. M. *J. Colloid Interface Sci.* **1981**, 83, 531.

(24) Xu, S.; Arnsdorf, M. F. *Proc. Natl. Acad. Sci. U.S.A.* **1995**, 92, 10384.

(25) (a) Hudson, J. E.; Abruna, H. D. *J. Am. Chem. Soc.* **1996**, 118, 6303; (b) Green, J.-B.; McDermott, M. T.; Porter, M. D. *J. Phys. Chem.* **1996**, 100, 13342.

photoelectron spectroscopy on both Si and Si<sub>3</sub>N<sub>4</sub> surfaces. Contact angles were measured using a Rame-Hart Model 100 goniometer at room temperature and ambient humidity (70% relative humidity (RH)).

**SAM Photopatterning.** Amines were covalently attached to Au-I SAM substrates in high yield by UV irradiation as previously reported.<sup>26</sup> SAMs terminating in two distinct functional groups were formed by double irradiation using a mask to define the pattern in the first step. To obtain a patterned surface terminating in a specific array of -COOH and -OH groups, a drop of ethyl 4-aminobutyrate was first placed on a freshly rinsed and dried Au-I substrate. A Cr-on-quartz mask was then placed on top of the substrate, Cr side down, forcing the amine to spread evenly across the sample. The assembly was irradiated for 2 min through the mask using a filtered (10 cm quartz cell filled with 1:1:1 H<sub>2</sub>O/EtOH/CH<sub>3</sub>COOEt) 200 W Hg lamp ( $\lambda > 260$  nm). After rinsing with a copious amounts of EtOH and drying with a stream of dry N<sub>2</sub>, a drop of diethanolamine was applied to the sample. A clear quartz plate was placed on the sample, and the assembly was uniformly irradiated for 2 min, rinsed, and dried. Patterned surfaces terminating in a COOH and CH<sub>3</sub> groups were obtained in a similar way, except that in the second irradiation step dibutylamine was used instead of diethanolamine.

The surface-confined ethyl ester was hydrolyzed following a procedure previously reported.<sup>12</sup> Before CFM imaging, the samples were cut into 1.2 cm  $\times$  1.2 cm squares, rinsed with DI H<sub>2</sub>O, and dried with a stream of dry N<sub>2</sub>. Freshly prepared samples were used for each set of experiments.

**Chemical Force Microscopy.** Adhesion and friction measurements were made with a Digital Instruments (Santa Barbara, CA) Nanoscope III multimode scanning force microscope equipped with a fluid cell. Modified tips were rinsed in EtOH and dried under N<sub>2</sub> just prior to mounting them in the fluid cell. Normal and lateral spring constants of triangular, 220  $\mu$ m long Si<sub>3</sub>N<sub>4</sub> cantilevers were obtained using methodology outlined previously.<sup>12</sup> Briefly, the normal spring constant of a cantilever was calibrated using a resonance endmass detection method.<sup>27</sup> Lateral spring constants were then obtained using the calculated ratio of lateral to normal spring constants.<sup>12</sup> The lateral sensitivity of the microscope optical detector was calibrated using a published procedure.<sup>28</sup> The values of the normal and lateral spring constants were  $0.10 \pm 0.02$  and  $188 \pm 38$  N/m, respectively. Tip radii were determined after CFM experiments from high-resolution scanning electron microscope images.

**CFM Data Analysis.** All force versus distance curves and lateral force traces were captured using Nanoscope III software and later analyzed on a Macintosh computer using a set of custom procedures written for Igor Pro2.04 data analysis software (WaveMetrics Inc, Lake Oswego, OR). Average adhesion force values were determined from histograms of the adhesion values obtained from at least 100 individual force versus displacement curves. The uncertainties ( $\pm 1$  standard deviation) in measured adhesion force values were  $\leq 0.5$  nN for small adhesion forces ( $< 8$  nN) between hydrophilic surfaces (COOH and OH) and increased to 2–5 nN for larger force values (30–60 nN) observed between hydrophobic surfaces. The adhesion force values could vary by up to a factor of 2 between similar samples, but agreed within 20–30% when normalized by the tip radii. The errors in surface free energy values determined from these data are reported on the basis of the widths of the adhesion distributions, but also are found to be representative of the errors determined by averaging of multiple experiments.

Repulsive double-layer force–separation curves were obtained after accounting for cantilever deflection away from the sample and represent averages from 20 individual measurements. These curves were fit with a double-layer model that uses linearized versions of Poisson–Boltzmann and surface charge–potential regulation equations and includes van der Waals attractive forces. In the case of 0.01 M ionic strength measurements, the force–distance curve can be fit reasonably well down to separations of 1.0 nm with a contribution from the van der Waals attractive force at short distances; in all other cases, curves

were fit down to separations of 0.5–1.0 nm before the jump in point. The accuracy of the numerical values of the surface potential is 20–30% due to high surface potentials found in these fittings ( $< -120$  mV) and uncertainty in the tip radius.

Friction force values were determined from lateral force traces, each containing 512 data points, by averaging the differences in friction forces observed when scanning over ca. 10  $\mu$ m distances in opposite directions at 80  $\mu$ m/s. Friction coefficients were found from linear fits to friction versus load curves containing 10–20 data points. Lateral force images were acquired and processed using Nanoscope III software.

## Results and Discussion

The dissociation constants of the surface acidic and basic groups often differ from those of their monomer analogs in solution. Several factors contribute to these differences, including (1) the presence of a low dielectric permittivity region surrounding the acidic or basic group, (2) changes in the number of degrees of freedom for the immobilized species, and (3) an excess electrostatic free energy of the supporting surface and change in the dielectric constant of the solution in the vicinity of a charged surface.<sup>29</sup>

The contact angle titration method is widely used as a simple approach to determining surface functional group pK values.<sup>30</sup> It is based on the fact that the surface free energy will depend on the ionization state of the functional group and on average will be representative of the degree of ionization. Experimentally, one expects to see an abrupt change in a contact angle at a pH corresponding to the pK of the surface group. This technique is, however, limited to surfaces sufficiently hydrophobic that they are not wet completely in both states. Alternatively, it has been suggested that the electrochemically-determined interfacial capacitance can be used to assess the pK of surface-confined groups in a completely wetted state,<sup>31,32</sup> although there is little experimental data available for direct comparison with these predictions.<sup>32</sup>

Chemically-modified AFM tips and samples can be used to probe directly changes in solid–liquid surface free energies with pH, and thus the dissociation constant of a surface-confined acid or base. A change in the surface charge induced by the dissociation of acidic (or protonated basic) groups can be detected by monitoring the adhesive force between the surface and an AFM probe modified with a chemical group sensitive to electrostatic interactions. Variations in the sign and magnitude of the force will indicate changes in the ionization state, and an abrupt transition will occur at a pH approximately equal to the pK of the functional group on the surface. Unlike contact angle titrations, the degree of surface wetting does not impact the ability to measure the pK; that is, both hydrophobic and hydrophilic surfaces can be studied.

**Adhesion Force and Contact Angle Titrations: Probing Local and Average Surface pK.** The adhesive interactions between tips and samples functionalized with different groups were determined by recording force versus distance curves. Such curves monitor the deflection of a probe cantilever as the sample and tip approach and subsequently separate from each other. The tip deflection is converted into a force using the tip–cantilever spring constant. The pull-off force in the withdrawal trace corresponds to the adhesion force. In general, force microscopy measurements include contributions from both chemical and mechanical properties of the materials being

(29) Zhmud, B. V.; Golub, A. A. *J. Colloid Interface Sci.* **1994**, *167*, 186.

(30) Holmes-Farley, S. R.; Reamey, R. H.; McCarthy, T. J.; Deutch, J.; Whitesides, G. M. *Langmuir* **1988**, *4*, 921.

(31) (a) Smith, C. P.; White, H. S. *Langmuir* **1993**, *9*, 1. (b) Fawcett, W. R.; Fedurco, M.; Kovacova, Z. *Langmuir* **1994**, *10*, 2403.

(32) Bryant, M. A.; Crooks, R. M. *Langmuir* **1993**, *9*, 385.

(26) E. W. Wollman; Kang, D.; Frisbie, C. D.; Lorkovic, I. M.; Wrighton, M. S. *J. Am. Chem. Soc.* **1994**, *116*, 4395.

(27) Cleveland, J. P.; Manne, S.; Bocek, D.; Hansma, P. K. *Rev. Sci. Instrum.* **1993**, *64*, 403.

(28) Liu, Y.; Wu, T.; Fennel-Evans, D. *Langmuir* **1994**, *10*, 2241.

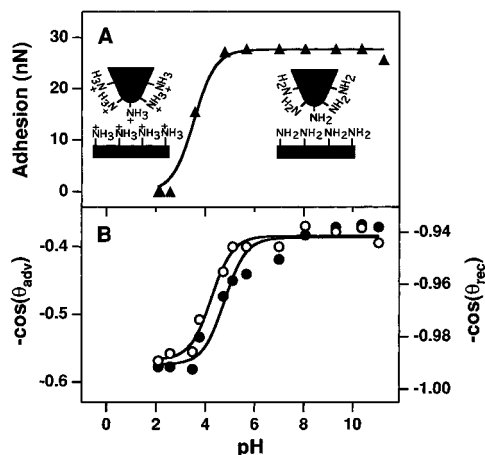


**Figure 1.** (A) Adhesion force between the sample and tip functionalized with amino groups versus pH. Adhesion force represents a mean value obtained from more than 200 single measurements. There was no time-dependent change observed during these measurements. The diagrams of the tip and sample show schematically the interfacial chemistry of the surface functionality; they do not accurately portray the hydrocarbon chain or true tip–sample contact area. (B) Negative cosines of the advancing (open circles) and receding (filled circles) contact angles of phosphate buffer drops on a sample modified with APTES as a function of pH.

studied. In our pH-dependent studies described below, mechanical contributions are effectively eliminated since the only change in the SAM is the degree of protonation of the outer functional group (i.e., the mechanical properties, which are determined by the hydrocarbon chain, are constant). Average adhesion force values obtained at different solution pH values (100 individual force measurements for each pH value) for tips and samples functionalized with APTES SAMs terminating with amine groups are plotted in Figure 1A. These data show that the adhesion force drops sharply to zero (indicating a repulsive interaction) below a pH of 4. The decrease and elimination of an attractive force between the tip and sample are consistent with protonation of the amine groups on these two surfaces. For comparison, we have measured contact angles using buffered solution droplets on this same surface (Figure 1B). These data also show a sharp transition (an increase in wettability) as the droplet pH is reduced below pH 4.5. An increase in wettability is expected when the surface becomes protonated. Hence, local force microscopy measurements using a modified probe tip and macroscopic wetting studies provide very similar values for the  $pK$  of the surface amine group in the APTES-derived SAMs. We term the AFM approach to determining local  $pK$  values “force titrations”.

The apparent  $pK$  obtained from force microscopy, 3.9, and contact angle wetting, 4.3, for the surface amine group is 6–7  $pK$  units lower than bulk solution values.<sup>33</sup> Large shifts in dissociation constants have been observed previously for mixed acid–methyl monolayers and attributed to unfavorable solvation of the carboxylate anion at the monolayer interface.<sup>34</sup> Large  $pK$  shifts relative to solution were also observed in studies of amino groups grafted onto the surface of a hydrophobic polymer.<sup>35</sup> In addition, recent simulations of the titration of surface amine groups showed large negative shifts in  $pK$  when the amine was poorly solvated.<sup>36</sup> The relatively high contact angles and large adhesion forces at  $pH > 4$  observed in our

experiments indicate that the APTES-derived monolayers are hydrophobic, since the interfacial tension in the alkylamine–water system is almost negligible ( $<0.1$  mJ/m<sup>2</sup>).<sup>37</sup> The hydrophobic nature of the SAM likely arises from a disordered structure that exposes methylene groups at the surface. Hence, we believe that it is reasonable to attribute the large observed  $pK$  shift to a hydrophobic environment surrounding the amine groups. The ability to detect such  $pK$  changes locally by AFM ultimately should be of significant utility in biological systems as well.

**Force Titrations Determine the Local  $pK$  of Hydrophilic Surfaces.** It is important to note that contact angle titrations cannot be used to determine the  $pK$  values of high-energy (hydrophilic) surfaces, because complete wetting and/or reactive spreading can occur in both the nonionized and ionized states of the system. In these high surface energy cases, it is necessary to dilute the hydrophilic groups with a hydrophobic surface component, and either to pretreat the surface<sup>34</sup> or use another liquid (vs vapor phase)<sup>38</sup> to perform the wetting experiment. As our previous results on the APTES system demonstrate, the incorporation of a hydrophobic component must be used with considerable caution, since it can produce very large  $pK$  shifts. Indeed, shifts in the  $pK_a$  of surface COOH relative to bulk solution have been observed in cases of mixed COOH and CH<sub>3</sub> SAMs.<sup>34,38</sup> Hence, it has not been possible to determine the  $pK$  of a homogeneous COOH-terminated surface by the contact angle approach.

Force titrations provide a direct measure of the solid–liquid interfacial free energy and thus bypass the above limitations. A force titration curve obtained for a COOH-terminated sample and COOH-terminated tip is shown in the Figure 2A. A prominent feature in this plot is the transition from a positive value of the adhesion force at low pH to zero (indicating repulsion) at high pH. This transition is relatively sharp and occurs within 2 pH units. The observed repulsion at  $pH > 6$  can be attributed to electrostatic repulsion between negatively charged carboxylate groups, while the adhesive interactions at low pH values originate from hydrogen bonding between uncharged COOH groups. The force versus separation curves become fully reversible and practically identical at all pH values higher than 7. This indicates that the surface charge density is saturated under these conditions (i.e., the carboxyl groups are fully deprotonated). On the basis of these titration data, we estimate the  $pK_a$  of the surface-confined carboxylic acid to be  $5.5 \pm 0.5$ . This value lies within 0.75  $pK$  unit from the value of  $pK_a$  for COOH functionality in aqueous solution.<sup>33</sup> The similarity of surface-confined and solution  $pK_a$  values strongly indicates that solvation effects do not play a significant role in determining the behavior of pure –COOH-terminated SAMs.

Control experiments with both hydrophilic and hydrophobic groups that do not dissociate in aqueous solutions did not display pH-dependent transitions. AFM titration curves for tip–sample SAMs terminating in OH/OH and CH<sub>3</sub>/CH<sub>3</sub> functionalities show (Figure 2B) an approximately constant, finite adhesion interaction throughout the whole pH range studied. Similar adhesion forces were also observed for these uncharged groups in DI H<sub>2</sub>O. It is worth noting, however, that the measured adhesion forces between CH<sub>3</sub>-terminated SAMs were typically 1–2 orders of magnitude larger than the forces observed for hydrophilic groups (COOH/COOH, OH/OH, COOH/OH). This large difference shows clearly the importance of hydrophobic forces in aqueous media, and are consistent with another recent

(33) CRC Handbook of Chemistry and Physics, 72nd ed.; Lide, D. R., Ed.; CRC Press: Boca Raton, FL, 1991.

(34) Creager, S. E.; Clark, J. *Langmuir* **1994**, *10*, 3675.

(35) Chatelier, R.; Drummond, C.; Chan, D.; Vasic, Z.; Gengenbach, T.; Griesser, H. *Langmuir* **1995**, *11*, 4122.

(36) Smart, J. L.; McCammon, J. A. *J. Am. Chem. Soc.* **1996**, *118*, 2283.

(37) Gliniski, G. C.; Platten, J. K.; De Saedeleer, C. J. *Colloid Interface Sci.* **1993**, *162*, 129.

(38) Lee, T. R.; Carey, R. I.; Biebuyck, H. A.; Whitesides, G. M. *Langmuir* **1994**, *10*, 741.

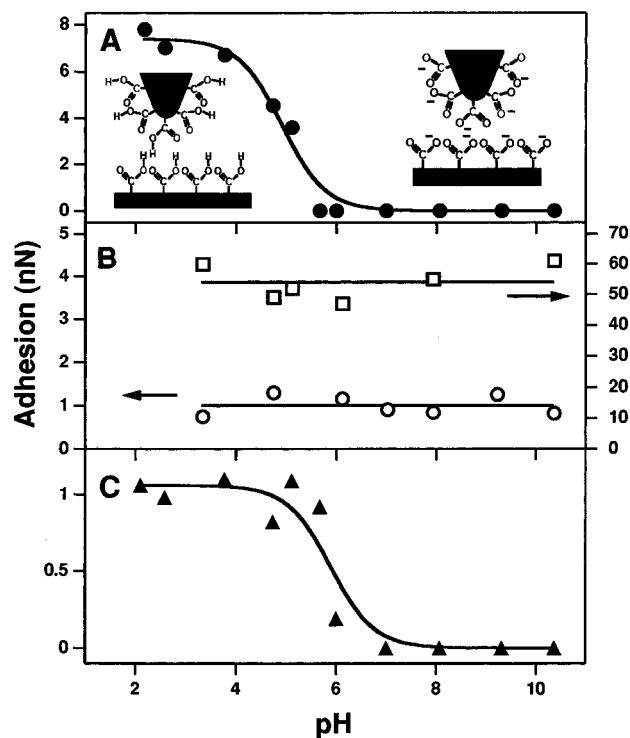


**Figure 2.** Adhesion force titration curves recorded in buffered solutions. Adhesion force versus pH for (A) COOH/COOH, (B) CH<sub>3</sub>/CH<sub>3</sub> (filled squares), OH/OH (filled circles), and (C) COOH/OH contacts. The diagrams of the tip and sample in (A) show schematically the interfacial chemistry of the surface functionality; they do not accurately portray the hydrocarbon chain or true tip-sample contact area.

CFM study.<sup>13e</sup> These data also support our conclusion that hydrophobic and solvation effects are responsible for the anomalously high adhesion force (and large shift in  $pK$ ) between APTES monolayers.

In addition, the widths of the transitions in our titration curves are quite typical of the corresponding solution titrations of a weak acid (base) with strong base (acid) and occur within 2 pH units. This is consistent with contact angle titration data on SAMs.<sup>34,38</sup> Solid lines in Figures 1 and 2 represent fits to solution-like titrations:  $\log[f/(1-f)] = \text{pH} - \text{p}K_a$ , where  $f$  is the degree of ionization at the surface. In these fits, the fraction of neutral groups is identified with the ratio of adhesion forces,  $F_{\text{adh}}(\text{pH})/F_{\text{adh}}(\text{pH} = 2)$ . In spite of the crudeness of the model and the neglect of electrostatic effects, the width of the transition is reproduced.

Lastly, in developing a general probe of  $pK$  values on unknown surfaces, it will be useful to use a functionalized SAM on the tip that (1) does not exhibit a pH-dependent change in ionization and (2) is hydrophilic. The hydroxyl-terminated SAM meets these requirements, and has been used to determine the  $pK_a$  of the carboxyl-terminated SAM as shown in Figure 2C. The dissociation constant is within 0.5  $pK$  unit of the value determined from the data in Figure 2A using  $-\text{COOH}$ -terminated SAMs on both the sample and tip. The slightly higher  $pK_a$  value in this case is expected, since the OH-terminated SAM remains uncharged. Therefore, the same magnitude of repulsive force is achieved at lower surface charge density (lower pH) in the case of overlapping double layers (COOH/COOH), than in the case of a double layer interacting with a neutral low dielectric constant surface (OH/COOH).

**Model and quantitative analysis.** In recent work,<sup>12</sup> we showed that the JKR theory of contact mechanics can serve as a reasonable basis for quantitative understanding of adhesion

data.<sup>3</sup> In this model, the force of adhesion  $F_{\text{adh}}$  is proportional to the work of adhesion  $W_{\text{st}}$  needed to separate the tip and sample surfaces:

$$F_{\text{adh}} = (3/2)\pi RW_{\text{st}} \quad (1)$$

The work of adhesion is given by

$$W_{\text{st}} = \gamma_s + \gamma_t - \gamma_{\text{st}} \quad (2)$$

where  $\gamma_t$  and  $\gamma_s$  are the surface free energies of the solvated tip and sample surfaces and  $\gamma_{\text{st}}$  is the free energy of the tip-sample interface. To interpret pH-dependent adhesion data for interactions in electrolyte solutions, we should include long-range electrostatic forces when considering the interaction between the tip and the surface. Since the JKR theory is based on energy balance, one expects no adhesion (Hertzian behavior) when the free energy of a double layer per unit area  $w_{\text{DL}}$  balances  $W_{\text{st}}$ . In quantitative terms, the pull-off force  $P_{\text{pull-off}}$  is related to these two terms:

$$P_{\text{pull-off}} = -(3/2)\pi RW_{\text{st}} + (5/2)P_{\text{DL}} \quad (3)$$

where  $P_{\text{DL}} = 2\pi GRw_{\text{DL}}$  is an additional load that has to be applied to a spherically shaped tip due to the presence of a double layer ( $G \approx 1.2$  is a geometrical factor for the deformed tip interacting at a constant potential). Thus, repulsion between like-charged surfaces ( $P_{\text{DL}} > 0$ ) will decrease the magnitude of the pull-off force compared to that given by the JKR theory. There is a threshold value of a repulsive electrical double layer force  $P_{\text{DL}} = P_0$ , beyond which the deformation of a spherical tip should be fully reversible with a contact radius going monotonically to zero (no pull-off force) as the load is reduced. This is equivalent to  $W_{\text{st}} = 2Gw_{\text{DL}} \approx 2w_{\text{DL}}$  (i.e., the attractive surface free energy component is canceled by the repulsive double layer term); the corresponding surface potential is then

$$\psi = [(\lambda/G\epsilon\epsilon_0)\gamma_{\text{SL}}]^{1/2} \quad (4)$$

independent of the tip radius for  $\lambda \ll R$  ( $\lambda$  is the Debye length).<sup>39</sup> Therefore, the change from adhesive to repulsive behavior is characteristic of the ionization state of the interacting surfaces and can be used to estimate the surface potential.

We have used the above model to calculate the surface free energies and surface potentials of the functionalized SAMs. The values of  $\gamma_{\text{SL}}$  determined from our adhesion data for OH and COOH (fully protonated) terminated surfaces were  $8 \pm 3$  and  $16 \pm 4$  mJ/m<sup>2</sup>, respectively. These values are in a good agreement with the values determined from interfacial tension measurements using two-phase systems consisting of water and melts of either long-chained alcohols<sup>40</sup> (7–8 mJ/m<sup>2</sup>) or carboxylic acids<sup>41</sup> (10–11 mJ/m<sup>2</sup>). We have also estimated the surface potential of the carboxylate SAM at pH 6 and  $I = 0.01$  M using eq 4. Our calculated value of  $-140 \pm 20$  mV is in reasonable agreement with an independent analysis of long-chain, fatty acid monolayers at the air-water interface under the same condition.<sup>42</sup> We further substantiate this result by analyzing our force-distance curves as discussed below.

**Probing Double-Layer Forces.** The electrostatic origin of pH-dependent repulsive forces can be verified by changing the Debye screening length  $\lambda$ .<sup>3,19</sup> We have varied  $\lambda$  by changing

(39) For our force titration experiments,  $\lambda = 3$  nm and  $R > 30$  nm.

(40) Gliniski, J.; Chavepeyer, G.; Platten, J. K.; Saedeleer, C. D. *J. Colloid Interface Sci.* **1993**, *158*, 382.

(41) Chavepeyer, G.; De Saedeleer, C.; Platten, J. *J. Colloid Interface Sci.* **1994**, *167*, 464.

(42) Yazdaniyan, M.; Yu, H.; Zograf, G. *Langmuir* **1990**, *6*, 1093.

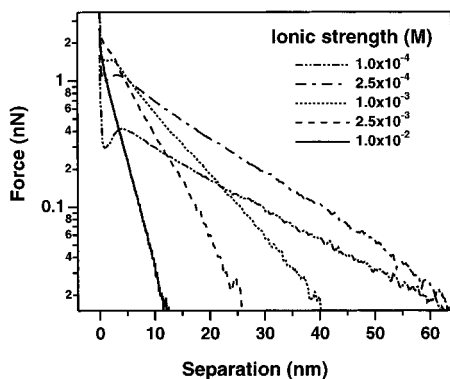


**Figure 3.** Repulsive double layer forces versus separation recorded upon approach between COOH-modified tips and samples at different solution ionic strengths. The pH in all of these measurements was 7.2. Each curve represents an average of 20 individual measurements.

the solution ionic strength. Figure 3A shows that the repulsive interaction becomes progressively longer-ranged as the solution ionic strength decreases. A detailed analysis of the electrostatic force is nontrivial due to the tip-sample geometry and the condition of surface charge-potential regulation imposed by the potential-dependent binding of  $H^+$  and  $Na^+$  ions at the interface. The surface charge-potential regulation has been observed previously in colloidal probe microscopy investigation.<sup>19</sup> This concept has been used in SFA studies to analyze double-layer interactions involving mica surfaces and 1:1 electrolytes.<sup>23</sup> *In situ* X-ray reflectivity measurements have shown that the interaction between monolayer carboxylate groups and divalent counterions can be sufficiently strong to form dense irreversibly bound overlayers.<sup>43</sup>

We have analyzed our data (Figure 3) using a model that takes the above factors into account.<sup>44</sup> In this model, the extent of charge regulation can be characterized by a single adjustable parameter  $\alpha$  ( $-1 \leq \alpha \leq 1$ ), where  $\alpha = 1$  corresponds to the limit of constant potential and  $\alpha = -1$  corresponds to the limit of constant charge. For the carboxylate surfaces studied in Figure 3 we find that the experimental data are well fit down to separations of 1 nm with a single value of  $\alpha$ ,  $-0.40 \pm 0.05$ , independent of ionic strength (Figure 4A). This analysis suggests that we approach the condition of constant charge (vs constant potential) in these experiments. The values of the screening length,  $\lambda_{exp}$ , extracted from experimental force versus separation curves agree well with the screening lengths,  $\lambda_{cal}$ , calculated from the ionic strength values for our experiments (Figure 4B). Significantly, the surface potential calculated using this analysis for the carboxy-terminated surface at pH 7.2 and 0.01 M ionic strength,  $-120 \pm 5$  mV, is close to the value estimated from adhesion measurements and discussed above. These results suggest that it may be possible to determine double-layer parameters of systems being imaged by simultaneously recording force versus distance curves. If these data are recorded using a tip bearing a functional group with a predetermined ionization behavior, the above analysis can provide double-layer parameters. In addition, analysis of surface potential data versus pH can yield the isoelectric point of a

(43) J. Li, Liang, K. S.; Scoles, G.; Ulman, A. *Langmuir* **1995**, *11*, 4418.

(44) The model makes use of the linearized surface charge-potential regulation condition, in which case an expression for potential energy of a two-plate system is

$$W_e = 2 \frac{\epsilon \epsilon_0 (\psi_{DL}^\infty)^2}{\lambda} \frac{\exp(-h/\lambda)}{1 + \alpha \exp(-h/\lambda)}$$

where  $\psi_{DL}^\infty$  is the diffuse double layer potential of an isolated surface. The details are given in Reiner, E. S.; Radke, C. J. *Adv. Colloid Interface Sci.* **1993**, *58*, 87.

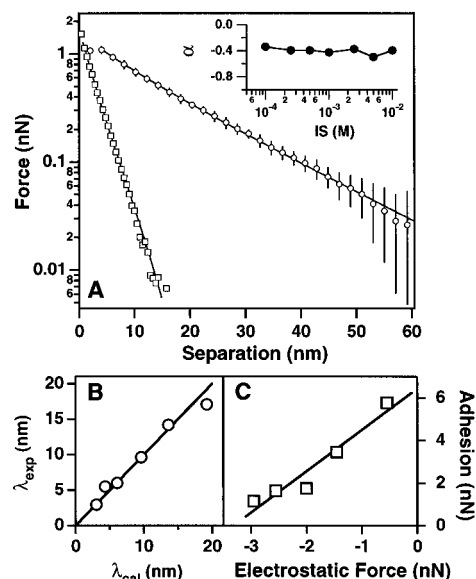


**Figure 4.** Theoretical fits (solid lines) with the double-layer model described in the text to experimental data on repulsive forces between  $COO^-/COO^-$  surfaces at pH 7.2 and  $I = 0.01$  M (squares) and  $0.00025$  M (circles). The number of experimental data points is reduced by a factor of 10 for clarity. The tip was treated as a square pyramid (apex half-angle  $35^\circ$ ) truncated with a hemisphere of  $R = 30$  nm. Error bars from averaging of multiple (20) force curves are shown for the data at  $I = 0.00025$  M and are representative of experimental error at all  $I$  values ( $\leq 0.05$  nN). Residuals determined for average values were  $\leq 0.01$  nN at all tip-sample separations and all  $I$  values studied. The inset shows the value of the adjustable parameter  $\alpha$  characterizing the degree of charge-potential regulation versus  $I$ . (B) Debye length obtained from experimental data and calculated from solution ionic strength. (C) Observed relationship between the adhesion force and repulsive electrostatic force,  $-P_{DL}$ , for COOH-terminated tips and samples.

sample (similar to the adhesion force titration); such experiments have been reported for silicon nitride tips on oxide surfaces.<sup>45</sup>

It is also evident in Figure 3 that the magnitude of the electrostatic force decreases for  $I < 1 \times 10^{-2}$  M at small tip-sample separations. Equivalently, the values of  $P_{DL}$ , which were determined from the above fits, decrease for  $I < 1 \times 10^{-2}$  M. These data contrast results obtained with a silicon nitride tip and mica sample,<sup>16b</sup> although more recent work<sup>46</sup> has shown that the surface charge of mica may undergo a sign reversal (as a function of  $I$ ) that complicates a direct comparison with our data. In addition, we find that adhesion can occur between surfaces despite the repulsive interaction; a plot of the measured adhesion force as a function of the electrostatic force is shown in Figure 4C. This phenomenon is fully reversible: by varying the ionic strength one can go from pure repulsion at high ionic strengths to repulsion on approach and adhesion on separation at low ionic strengths. A decrease in ionic strength (larger  $\lambda$ ) will diminish the double-layer repulsion (ref 44 and Figure 3), and according to eq 3 this should result in a larger adhesion force as found in Figure 4C.

Lastly, we can estimate the number of species involved in double-layer interactions. For a tip with a radius of  $R = 30$  nm in contact with the sample surface in solution of 0.01 M ionic strength, there are more than 200 ions and  $1 \times 10^6$  water molecules involved in the interaction! This contrasts the situation in organic solvents where there are typically only 15–

(45) (a) Arai, T.; Fujihira, M. *J. Vac. Sci. Technol. B* **1996**, *14*, 1378.

(b) Arai, T.; Fujihira, M. *J. Electroanal. Chem.* **1994**, *374*, 269.

(46) Kekicheff, P.; Marcelja, S.; Senden, T. J.; Shubin, V. E. *J. Chem. Phys.* **1993**, *99*, 6098.

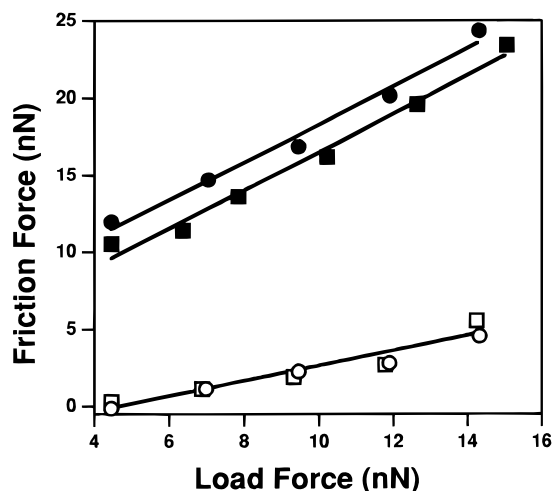


**Figure 5.** Frictional force versus applied load curves for COOH/COOH functionalized tips and samples recorded at pH 2.2 and 3.5 (filled circles and squares) and pH 7.0 and 9.3 (open circles and squares).

25 molecular contacts.<sup>12</sup> Thus, when using repulsive electrostatic forces in constant force imaging, one has to keep in mind that these forces are averaged over relatively large sample areas.<sup>45,47</sup>

**Friction Measurements.** The lateral friction force was measured by recording traces of cantilever lateral deflection (“friction loops”)<sup>48</sup> while the sample was rastered back and forth using the piezo scanner. The resulting lateral deflection traces were converted to forces using the lateral spring constant for the AFM tip.<sup>12</sup> The external applied load was controlled independently through the cantilever normal deflection. Friction versus load curves were obtained from these data, and friction coefficients were determined from the slopes of these plots. Figure 5 shows typical friction versus load curves that were obtained using tip–sample combinations functionalized with carboxyl-terminated SAMs; the data were recorded at pH values where the carboxyl groups are protonated (2.2 and 3.5) and deprotonated (7.0 and 9.3). These friction data exhibit a linear increase with applied load as observed previously in ethanol<sup>12</sup> and argon.<sup>13a</sup> The increase in friction force arises from an increase in the tip–surface contact area with increasing applied load.<sup>1</sup> Significantly, the friction data in Figure 5 fall into two groups. Measurements made at pH values <5.5 yield higher friction forces and greater friction coefficients than measurements made at pH values >6.5. This crossover in behavior occurs at the same region of pH where the adhesion (normal) force exhibits a transition from attraction to repulsion (Figure 2A). In addition, there is a finite load (≈4 nN) necessary to achieve nonzero friction at high pH, since the double-layer repulsion must be overcome to bring the tip in physical contact with the sample surface. pH-dependent frictional forces were also observed for Si<sub>3</sub>N<sub>4</sub> tips on Si surfaces.<sup>49</sup> In this work, it was suggested that the protonation/deprotonation of surface Si–OH groups gave rise to observed changes in friction.

In addition, we have characterized systematically as a function of pH the friction versus load behavior of tips and samples functionalized with ionizable and nonionizable SAMs. These results are summarized in plots of the friction coefficient versus pH in Figure 6. The friction coefficients determined for –OH and –CH<sub>3</sub> (not shown) terminated SAMs are independent of

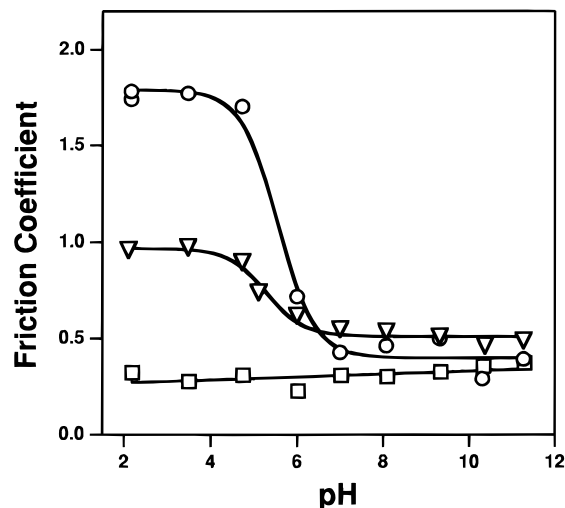


**Figure 6.** Friction coefficient versus pH for COOH/COOH (open circles), COOH/OH (open triangles), and OH/OH (open squares) contacts.

pH. These results are consistent with our expectations for nonionizable hydrophilic and hydrophobic groups, and are consistent with pH-independent adhesion forces observed for these functional groups (Figure 2). The friction coefficients determined for cases in which one or both SAM surfaces terminate in carboxyl groups show significant decreases at pH ≈ 6. These friction coefficient results thus exhibit similar pH dependencies to those observed in adhesion measurements. These results suggest that the drop in friction coefficient can be ascribed to the dissociation of protons from the surface carboxyl groups.<sup>50</sup> It is also interesting to note that at high pH the friction coefficient for COO<sup>−</sup>/OH surfaces is greater than that observed for COO<sup>−</sup>/COO<sup>−</sup>, while the reverse is true at low pH when the carboxyl groups are protonated. These results indicate that it should be possible to distinguish unambiguously surface –OH and –COOH functionality through pH-dependent imaging.

We also found that the magnitudes of the friction force and friction coefficient for hydroxyl-terminated surfaces were the lowest of those investigated in aqueous solution. Analysis of friction versus load curves for methyl-terminated tip–sample combinations also yielded low friction coefficients (~0.3); however, the magnitude of the friction force was at least an order of magnitude greater (~60 nN) than that of either carboxyl- or hydroxyl-functionalized surfaces. The large magnitude of the friction force between methyl surfaces in aqueous media can be attributed to the large contact area that occurs between hydrophobic surfaces. When the friction force is scaled by the contact area, it is apparent that the friction force per methyl group is smaller than the friction force per carboxyl group.

**CFM Imaging.** Recently we showed that lateral force imaging with chemically-modified tips can be used to map the spatial distribution of functional groups on surfaces.<sup>11,12</sup> In light of the above differences in friction observed for interactions between different functionalities in aqueous solutions, it should also be possible to generate hydrophobicity maps and ionization state specific maps of functional groups on surfaces. To test this idea, we have used a photochemical method to fabricate

(47) (a) Manne, S.; Cleveland, J. P.; Gaub, H. E.; Stucky, G. D.; Hansma, P. K. *Langmuir* **1994**, *10*, 4409. (b) Manne, S.; Gaub, H. E. *Science* **1995**, *270*, 1480.

(48) Overney, R. M.; Takano, H.; Fujihira, M.; Paulus, W.; Ringsdorf, H. *Phys. Rev. Lett.* **1994**, *72*, 3546.

(49) Marti, A.; Hahner, G.; Spencer, N. D. *Langmuir* **1995**, *11*, 4632.

(50) The lower magnitude of friction forces at constant load observed in ref 49 for higher pH should be predominantly attributed to a decrease in the effective (actual) normal load, because of a buildup of the repulsive double-layer force. Some change in a friction coefficient, however, can also be detected in friction force versus normal force curves presented in that work.

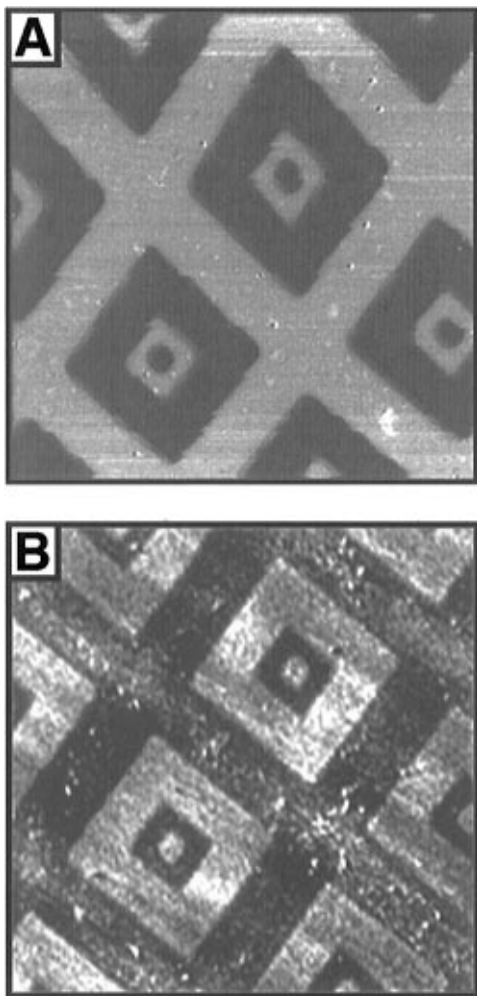


**Figure 7.** Lateral force image of a sample patterned with regions terminating in  $-\text{CH}_3$  and  $-\text{COOH}$  functional groups recorded in (A) DI water and (B) air with a methyl-functionalized tip. (A) Light regions are areas of high friction and correspond to surface regions terminating in  $\text{CH}_3$  functionality. Dark regions represent low friction and correspond to the surface areas terminating in  $\text{COOH}$  functional groups. (B) The high friction (light) areas correspond to regions terminating in  $-\text{COOH}$  groups, while the low friction (dark) areas correspond to the  $-\text{CH}_3$ -terminated regions. Both images correspond to  $100\ \mu\text{m} \times 100\ \mu\text{m}$  areas.

SAMs that have a repeating pattern of two regions that terminate in distinct functional groups.<sup>12</sup> These surfaces exhibited flat topography in AFM images, although small adventitious particles were often detected on the surfaces. This flat topography was obtained with both unmodified and modified tips independent of the functional groups on the tip.<sup>51</sup>

**Hydrophobic/Hydrophilic Patterned Surfaces.** Figure 7 shows lateral force images acquired using a  $\text{CH}_3$ -functionalized tip on surfaces that have a pattern of  $\text{COOH}$ -terminated regions repeating regularly on a  $\text{CH}_3$ -terminated background; the images were obtained in DI  $\text{H}_2\text{O}$  (Figure 7A) and air (Figure 7B). The friction contrast between  $-\text{COOH}$  and  $-\text{CH}_3$  functional groups is relatively large in both images. The contrast obtained in water on the  $\text{CH}_3/\text{COOH}$  pattern shows high friction in the methyl-terminated regions and low friction over the carboxyl-terminated

regions of the sample (Figure 7A). This result is readily understood from our friction studies discussed above; that is, the contrast reflects the dominant effect of hydrophobic forces that mask other chemical interactions. We suggest that imaging under water with hydrophobic, methyl-terminated tips or  $-\text{OH}$ -terminated tips should represent approaches that can be used to construct hydrophobicity maps of sample surfaces. Images acquired in air exhibit friction contrast that is inverted relative to the data obtained in aqueous solution (Figure 7B). This reversal in friction contrast does not reflect directly chemical interactions, but rather is due to large capillary forces between the sample and tip over the hydrophilic  $-\text{COOH}$ -terminated regions of the surface (which are wet more readily than  $-\text{CH}_3$ -terminated regions).

**pH-Sensitive Imaging of Patterned Surfaces.** In addition, we have imaged  $\text{COOH}/\text{OH}$  patterned surfaces with a  $\text{COOH}$ -terminated tip at different pH values. Figure 8 shows that the friction contrast between  $\text{COOH}/\text{OH}$  regions ( $\text{OH}$  groups in the background) is inverted as the pH is increased from 2.2 to 10.3 (the change in contrast occurs near pH 5–6 at the  $\text{p}K_a$  of the surface carboxyl). In addition, we note that all four images were taken with the same  $-\text{COOH}$ -modified tip over the same region of the surface, and that the actual order in which the images were recorded was A–D–C–B; i.e., the contrast reversed twice during the series of images. Further studies show that these pH-dependent changes are quite reversible. Because these image contrast changes occur at the pH point where the  $-\text{COOH}$  functional groups deprotonate (determined by adhesion measurements), we conclude that images such as Figure 8 represent rationally interpretable spatial maps of the ionization state of functional groups.

It is important to note that images of the  $\text{COOH}/\text{OH}$  patterned sample obtained with an unmodified  $\text{Si}_3\text{N}_4$  tip in acidic and basic pH solutions showed the same contrast (acid-terminated regions yielded a higher friction force than  $\text{OH}$ -terminated regions), and did not show pH-dependent contrast as observed with our functionalized tips. In addition, the contrast obtained with bare  $\text{Si}_3\text{N}_4$  tips was also lower than comparable radii modified tips. It is known that friction images of heterogeneous surfaces can be obtained with unmodified AFM tips;<sup>52</sup> however, the functionality and surface energy of these tips are somewhat uncontrolled since (1) the density of  $-\text{OH}$  groups can vary and (2) the tips can be easily contaminated with adsorbates.<sup>53</sup> Therefore, to use bare  $\text{Si}_3\text{N}_4$  tips as chemical sensors requires extensive cleaning,<sup>54</sup> and ultimately, does not offer the sensitivity and versatility that can be achieved through chemical modification.

Lastly, it is important for practical applications to consider imaging resolution. We believe that the present resolution of our images ( $\sim 100\ \text{nm}$ ) reflects the resolution of the photopatterning technique employed to prepare the patterned SAM surfaces and does not reflect the true resolution of CFM. The true resolution will be determined by the actual tip–sample contact area. An independent study recently showed that CFM can image functional group distributions with at least a resolution of  $10\ \text{nm}$ .<sup>13a</sup> We believe that by reducing the tip radius it should ultimately be possible to achieve a resolution of  $1\ \text{nm}$ . To carry out measurements with a spatial resolution

(51) A recent report claimed the observation of pseudoheight contrast dependent on the AFM tip functionality.<sup>13d</sup> We attribute it to strong height–friction coupling unavoidable in AFM experiments if the tip is scanned parallel to the cantilever axis of symmetry (see: Radmacher, M.; Tillman, R. W.; Fritz, M.; Gaub, H. E. *Science* **1992**, *257*, 1900. Warmack, R. J.; Zheng, X.-Y.; Thundat, T.; Allison, D. P. *Rev. Sci. Instrum.* **1993**, *65*, 394). In our experiment the tip was scanned in the perpendicular direction which eliminated the coupling.

(52) (a) Overney, R. M.; *et al. Nature* **1992**, *395*, 133. (b) Overney, R. M.; Meyer, E.; Frommer, J.; Guntherodt, H.-J.; Fujihira, M.; Takano, H.; Gotoh, Y. *Langmuir* **1994**, *10*, 1281. (c) Wilbur, J.; Biebuyck, H. A.; MacDonald, J. C.; Whitesides, J. M. *Langmuir* **1995**, *11*, 825.

(53) We found that when bare  $\text{Si}_3\text{N}_4$  tips are used for imaging of patterned surfaces in fluids, the image contrast is very often unpredictable and even changes during scanning.

(54) Thundat, T.; Zheng, X.-Y.; Chen, G. Y.; Sharp, S. L.; Warmack, R. J. *Appl. Phys. Lett.* **1993**, *63*, 2150.

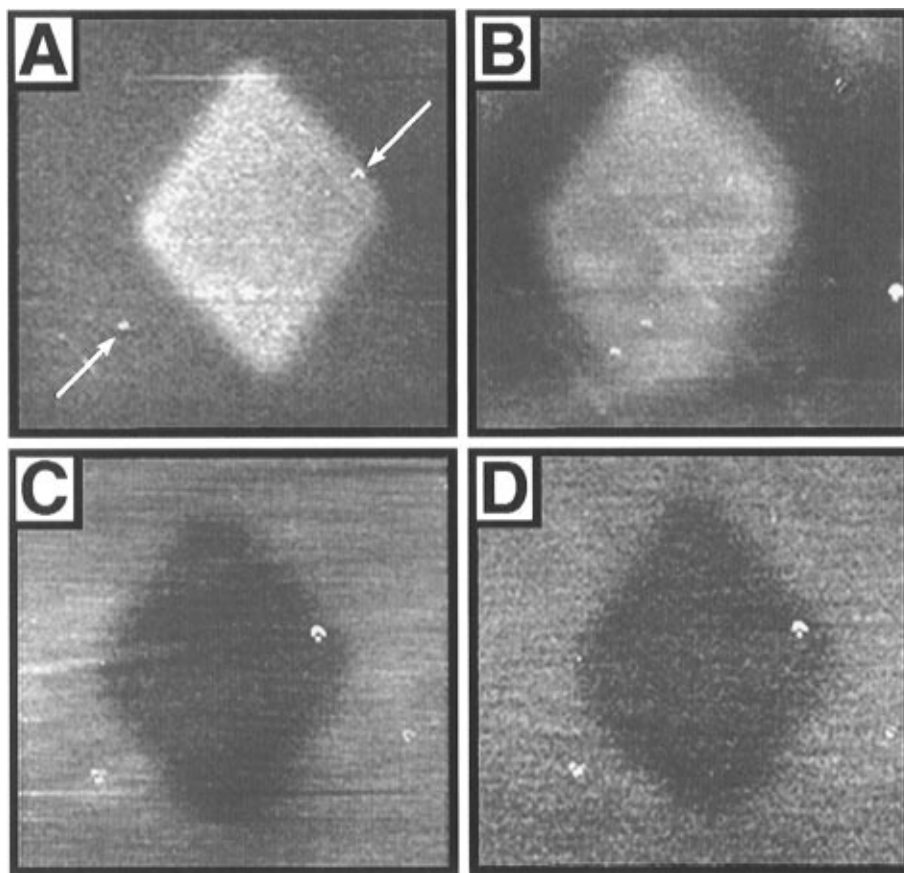


**Figure 8.** Lateral force images of the same region of a patterned SAM sample where the inner square terminates with  $-\text{COOH}$  groups and the surrounding background with  $-\text{OH}$  groups. The images were recorded with pH values of (A) 2.2, (B) 4.8, (C) 7.2, and (D) 10.3. Two particles are highlighted by arrows on image A and also can be seen in images C and D. Each of the four images correspond to  $30\ \mu\text{m} \times 30\ \mu\text{m}$  areas.

of 1 nm, it will be necessary to use tips with radii of a comparable scale. As estimated in our previous work,<sup>12</sup> 1 nm resolution can be achieved with a tip radius of  $\sim 8$  nm, if the surface forces are relatively small (i.e.,  $\gamma \approx 2$  mN/m). Currently, commercial AFM tips with radii on the order of 10 nm are available, and a recent report demonstrating the fabrication of carbon nanotube tips suggests that much smaller radii should be possible.<sup>55</sup> Strategies to modify chemically these tips while preserving their sharpness must, however, be developed. In addition, other imaging techniques will likely be needed to study biological samples. Two possibilities are adhesion force mapping and small deformation tapping. Adhesion force mapping is an obvious (but slow) extension of our adhesion measurements. Our ongoing work suggests that the general CFM approach to functional group mapping can also be adapted to tapping mode imaging when sample deformations are minimized.<sup>56</sup> Hence, we believe that CFM will lead to unique opportunities for chemists and biologists for nanoscale mapping of functional group distributions and ionization states in polymeric and biological systems.

## Conclusions

We have shown that AFM tips chemically-modified with SAMs terminating in a specific chemical functionality can be used to probe electrostatic forces and dissociation reactions in an aqueous medium. Adhesion force titration curves, analogous to conventional homogeneous solution pH titration curves, were shown to be a highly-sensitive and local probe of the  $\text{p}K$  values of surface functional groups. Adhesion measurements made

as a function of pH on amine-terminated surfaces exhibited a sharp decrease in the adhesion force at pH values below 4.5 and led to an estimated  $\text{p}K$ , 3.9, that was similar to the value determined by conventional contact angle wetting studies of the same surface. The large decrease in  $\text{p}K$  of the amine group relative to that of the homogeneous solution was attributed to the relatively hydrophobic environment of the amine group in these SAMs. Adhesion force titrations carried out on  $-\text{COOH}$ -terminated surfaces showed that the surface  $\text{p}K$ , 5.5, was similar to the free aqueous solution value for this hydrophilic surface. The interactions observed between the modified tip and sample surface were also shown to agree well qualitatively and quantitatively with the predictions of double-layer and modified JKR models. With these models we showed that CFM data can be used to extract surface free energies and double-layer parameters that are essential to understanding interactions with charged and uncharged surfaces in aqueous media.

Lateral forces between chemical functional groups in aqueous solutions were also found to be chemically specific. Friction force measurements made as a function of pH between tips and samples modified with SAMs terminating in  $-\text{COOH}$ ,  $-\text{OH}$ , and  $-\text{CH}_3$  groups exhibited a linear dependence on load with the slope corresponding to the coefficient of friction. The coefficient of friction for  $-\text{OH}$  and  $-\text{CH}_3$  groups was independent of pH, while the friction coefficient for  $-\text{COOH}$ -terminated surfaces decreased significantly at a pH corresponding to the  $\text{p}K_a$  determined by adhesion measurements. When present, hydrophobic effects dominate both adhesion and friction forces. Thus, the contrast observed in lateral force images taken with a hydrophobic tip can serve to map the hydrophobicity of a sample. On hydrophilic surfaces, however, the observed pH-dependent changes in friction forces of ionizable groups were

(55) Dai, H.; Hafner, J. H.; Rinzler, A. G.; Colbert, D. T.; Smalley, R. E. *Nature* **1996**, *384*, 147.

(56) Noy, A.; Vezenov, D.; Lieber, C. M., Manuscript in preparation.

exploited to map spatially surfaces terminating in  $-\text{COOH}$  and  $-\text{OH}$  functional groups. Hence, CFM can be used to image rationally the ionization state of surface groups.

It is also worth considering possible applications of CFM to chemistry and adjacent fields. Our approach of using force titrations to determine the local  $\text{p}K$  of acidic and basic groups may be applicable to probing the local electrostatic properties of protein surfaces in their native environments and the ionization of colloidal particles on the nanoscale. Adhesion force measurements between different surfaces in different media can also provide a wealth of thermodynamic data that are essential to understand and control intermolecular interac-

tions. Friction studies utilizing chemically-modified tips should also provide useful insight into the molecular mechanisms of dissipative processes such as friction and wear. Lastly, from an imaging standpoint it is now important to assess the applicability of CFM to more complex systems such as biological membranes and polymer surfaces.

**Acknowledgment.** C.M.L. acknowledges support of this work by the Air Force Office of Scientific Research (Grant F49620-94-1-0010) and the Office of Naval Research (Grant N0014-94-1-0004).

JA963375M